Method of Determining the Thickness and Uniformity of Application for Thermoplastic Pavement Marking Material

Report 0-4282-2

Prepared for
Texas Department of Transportation

By
Richard Liu
Jing Li
Xuemin Chen
Yuanhang Chen
Huichun Xing
Renyue Liang

Department of Electrical and Computer Engineering
University of Houston
Houston, Texas

October 2002

1. Report No. TxDOT 0-4282	2. Government Accession No.	3. Recipient's Catalog No.
4. Title and Subtitle Method of Determining the Thickness and Uniformity of Application for Thermoplastic Pavement Marking Material		5. Report Date October 2002
		6. Performing Organization Code
7. Author(s) Richard Liu, Jing Li, Xuemin Chen,Yuanhang Chen, Huichun Xing and Renyue Liang		8. Performing Organization Report No.
9. Performing Organization Name and Address Department of Electrical and Computer Engineering University of Houston 4800 Calhoun Rd. Houston, TX 77204-4005		10. Work Unit No.
		11. Contract or Grant No.
12. Sponsoring Agency Name and Address Research and Technology Implementation Office Texas Department of Transportation P. O. Box 5080 Austin, TX 78763-5080		13. Type of Report and Period Covered Final Report
		14. Sponsoring Agency Code

15. Supplementary Notes
    Project conducted in cooperation with the Texas Department of Transportation and the Federal Highway Administration

16. Abstract:

A laser thickness-measurement device for measuring the thickness of thermoplastic pavement marking material (TPMM) has been successfully developed. The system has been installed onto a pushcart for easy field operation. The device is based on a laser triangulation measurement system and it uses a position sensitive device (PSD) as the detector. The hardware developed includes a laser thickness detector, mechanical scanner, angle encoder, distance encoder, global positioning system (GPS) and interface circuitry, data acquisition and control circuitry, and data display. Software functions developed include data processing, embedded computer control, data filtering and the user interface. The system operates at a sampling rate of 175 kHz, which significantly increases the accuracy and speed of the thickness measurement and provides more quantitative information for determination of the TPMM and pavement profiles. The flexible hardware design enhances the system's performance under varied pavement conditions. The high response frequency allows the system to quickly adapt to sudden changes in slope and color. Lab and field tests demonstrated that the measured thicknesses were very close to the actual thickness of the tapes measured. Measurement error on smooth pavements (asphalt and concrete) was less than 5 mils. Measurement error on grade 3 surface treatments was within 10 mils.

17. Key Words Laser, laser triangulation, position sensitive device, thermoplastic, marking material, GPS		18. Distribution Statement No restrictions		
19. Security Classif. (of this report) Unclassified	20. Security Classif. (of this page) Unclassified	21. No. of Pages	22. Price	

Form DOT F 1700.7 (8-72)   Reproduction of completed page authorized

I

Final Report

Method of determining the thickness and uniformity of application for thermoplastic pavement marking material

Richard Liu

Associate Professor, Principle Investigator

Xuemin Chen

Research Assistant Professor

Jing Li

Research Associate

Yuanhang Chen

Huichun Xing

Renyue Liang

Research Assistants

DISCLAIMERS

The contents of this report reflect the views of the authors who are responsible for the facts and accuracy of the data presented herein. The contents do not necessarily reflect the official views or policies of the Texas Department of Transportation. This report does not constitute a standard, specification or regulation.

University of Houston

Houston, TX 77004

Table of Contents

List of Figures

VII

List of Tables

CHAPTER 1: INTRODUCTION

1.1 PROJECT BACKGROUND AND OVERVIEW

Currently, TxDOT measures the thickness of marking materials on pavement using a pre-embedded plate and measures the thickness after the spray of the TPPM. This method is accurate and efficient but labor intensive. A high-speed, non-invasive, preferably vehicle-mounted device is desirable to measure the TPPM. TxDOT uses tons of marking materials per week and monitoring the thickness becomes a very important issue. Due to the limited manpower in TxDOT, it is difficult to monitor all the contractors using the embedded plate method. On the other hand, the embedded-plate method cannot obtain a continuous-thickness profile.

Pavement-marking materials are made of thermoplastic with about 20-30% glass beads to increase reflectivity. Glass beads can either be spread on the top of the thermoplastic immediately after the spray, mixed with the thermoplastic, or both. Thermoplastic materials are heated to about 400 degrees and spread onto the pavement surface. The average thickness of the pavement marking materials on the smooth surface is about 0.3cm – 1.25 cm. However, for the rough pavement surface, e.g., TPPM on gravel, the thickness of marking materials becomes non-uniform because of the porosity between grains of rocks. The average grain size of surface rocks ranges from 1/4'' to about 1.5'' in diameter and they are irregularly shaped. Figure 1.1 shows a sample of marking material over pavement gravel. It is clearly shown that the marking materials flow into the pore space between rock grains. To measure the thickness of the marking materials in such cases, a non-contact method must be used, and some kind of averaging method must be applied.

Considering the required accuracy, in this project a laser-based thickness-measuring device for thermoplastic pavement marking material has been successfully developed. This device is based on the laser triangulation measurement using a position sensitive device (PSD) as detector. This system has a sampling rate of 175kHz, which greatly increases the accuracy of TPPM thickness measurement and provides quantitative

1

information for continuous profiling. The flexible hardware design enhances the system's performance under various practical situations; especially the high response speed which makes the system control more prompt in handling the abrupt changes in slopes and colors. This prototype includes laser transceivers, laser-beam scanning system, data acquisition system, global position system, distance-measuring device and associated software. Lab and field tests have been performed. The experiment results are very close to real thickness of thermoplastic.

Figure1.1 Sample of marking material over rocks

CHAPTER 2: THE LASER THERMOPLASTIC THICKNESS MEASUREMENT SYSTEM

2.1 SYSTEM GENERAL DESCRIPTION

The developed laser thickness device is a prototype device for measuring the thickness of marking materials on pavement by using laser technology. The device consists of two parts: a hardware system for measuring TPPT using a laser scanning technique and a software package to analyze and process the measured data. Figure 2.1 shows the structure of the pushcart that hosts the measurement system. The pushcart measures 42.5 inches in length, 29 inches in width, and 47 inches in height, respectively. The standoff distance defined between laser transmitter and ground is 12 inches.
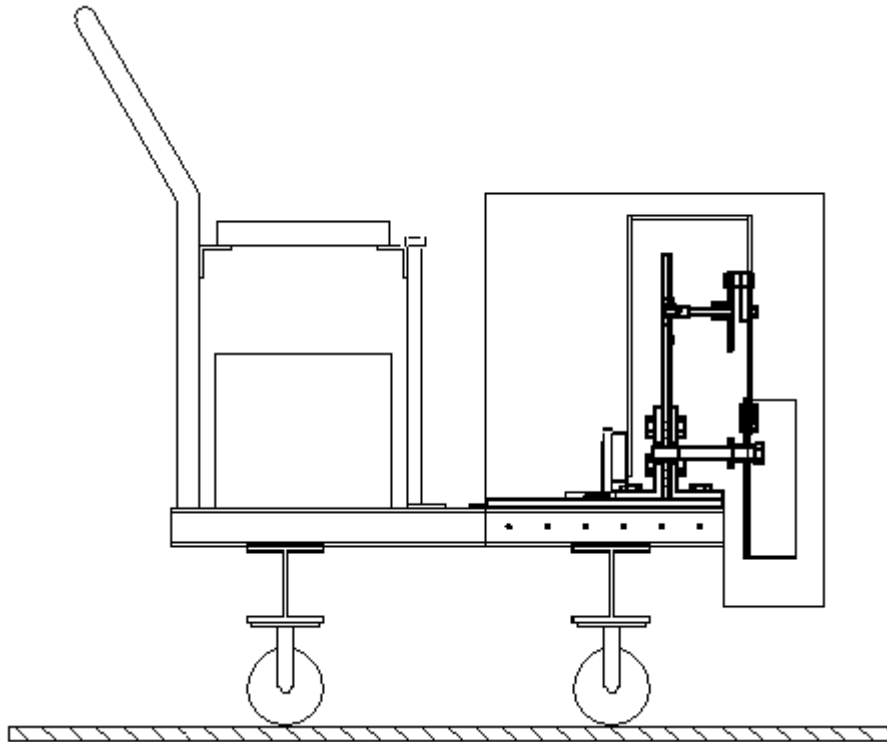
Figure 2.1 Designed pushcart structure

To describe the architecture of the device, a hardware block diagram is illustrated in Figure 2.2. The developed prototype device is shown in Figure 2.3.
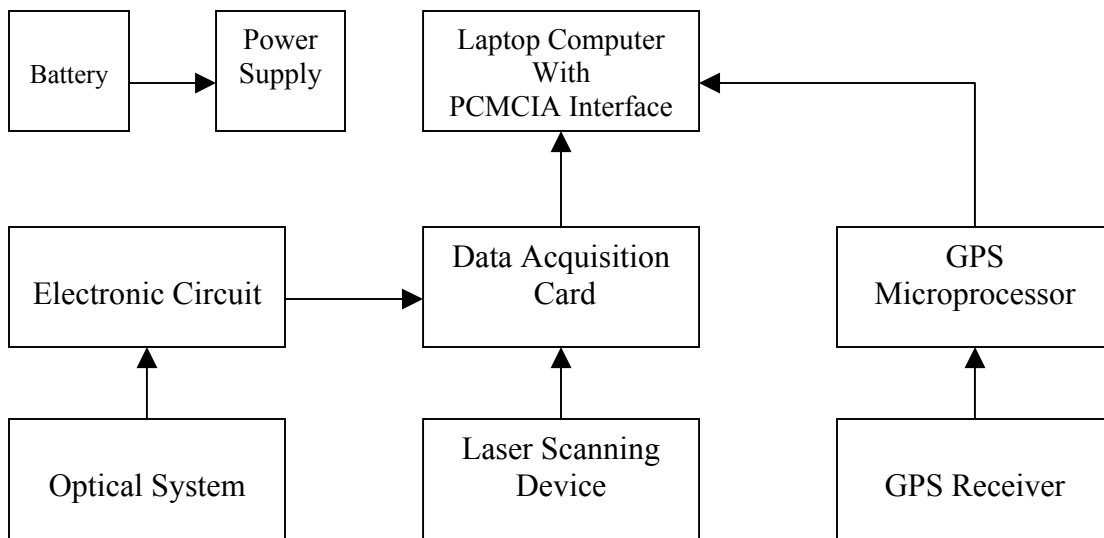
Figure 2.2 A block diagram of the hardware system

Figure 2.3 Prototype device for thermoplastic thickness measurement

CHAPTER 3: OPTICAL SYSTEM

3.1 OPTICAL SYSTEM DESIGN

The laser-based triangulation method is a distance measurement method and is adopted to provide simplicity, flexibility and high-speed operation. In this chapter, the discussion is focused on the implementation theory of the triangulation method.

3.1.1 INTRODUCTION

The triangulation method is a widely used approach in profiling, especially in surface inspection [1,2,3] due to the advantages of low cost, simplicity, robustness and high resolution [2-23]. There are several parameters pertaining to a range sensor that determines system performance. These parameters include sampling rate, dynamic range of depth measurement and measurement resolution (accuracy).

The laser-based triangulation system consists of a laser diode, an optical positioning system, a signal generation circuitry and a data acquisition and analysis system.

3.1.2 TRIANGULATION PRINCIPLE

Two components constitute the optical system of the triangulation range sensor: the laser beam generator and the position sensitive detector (PSD). In the following sections the mathematical formation of the triangulation method is presented.

Figure 3.1. Laser-based triangulation system

The concept of optical triangulation is illustrated in Figure 3.1. In Figure 3.1, a collimated laser beam illuminates the measurement surface. The target surface reflects the beam, which is then focused on the PSD forming a beam spot. The beam spot moves on the PSD as the surface height changes. The displacement of the surface can then be determined by detecting the movement of the beam spot.

Figure 3.2 Triangulation principle

Figure 3.2 illustrates the geometry of image formation on PSD. Assume that the laser beam intercepts the optical axis at point A and the virtual image of A is located at point C (on the axis). Image B corresponds to point D. According to the law of image focusing, the following relationships can be established:

$$\frac{1}{f} = \frac{1}{L} + \frac{1}{L'} \tag{3.1}$$

and

$$\frac{1}{f} = \frac{1}{L - H\cos\alpha} + \frac{1}{X}, \tag{3.2}$$

where H is the change of height (from point A to point B) and α is the formation angle (viewing angle) of the image. From Equations (3.1) and (3.2), L′ and X can be expressed as Equation (3.3) and Equation (3.4)

$$L' = \frac{Lf}{L - f} \tag{3.3}$$

and

$$X = \frac{f(L - H\cos\alpha)}{L - H\cos\alpha - f}. \tag{3.4}$$

The heights of point B and its image D comply with the law of image magnification, which is stated as Equation (3.5)

$$\frac{d}{H\sin\alpha} = \frac{X}{L - H\cos\alpha}. \tag{3.5}$$

where d is the height of the image. Substitute X using Equation (3.4), then d can be expressed as:

$$d = \frac{fH \sin\alpha}{L - H \cos\alpha - f} \ . \tag{3.6}$$

To find out α', the angle of PSD with the main optical axis, have

$$X - L' = \frac{f(L - H \cos\alpha)}{L - H \cos\alpha - f} - \frac{fL}{L - f}$$

$$= \frac{f^2 H \cos\alpha}{(L - f)(L - H \cos\alpha - f)} \ . \tag{3.7}$$

The slope of line segment CD therefore is

$$\tan\alpha' = \frac{d}{X - L'} = \frac{fH \sin\alpha}{L - H \cos\alpha - f} \times \frac{(L - f)(L - H \cos\alpha - f)}{f^2 H \cos\alpha'}$$

$$= \frac{(L - f)}{f} \tan\alpha$$

$$= const. \tag{3.8}$$

The position data p can be read out directly from the circuitry output. From Equation (3.9)

$$\frac{1}{f} = \frac{1}{H \sin\alpha} + \frac{1}{p \sin\alpha'} \ , \tag{3.9}$$

H can be calculated by Equation (3.10)

$$H = \frac{fp \sin\alpha'}{(p \sin\alpha' - f) \sin\alpha} \tag{3.10a}$$

or

8

$$p = \frac{Hf \sin \alpha}{(H \sin \alpha - f) \sin \alpha'}$$ (3.10b)

In the optical system design, two factors need to be taken into account: the choice of the imaging lens and the distance between the imaging lens and the object. The intensity of the reflected light is very weak (in μW). To increase the energy from the reflected light, a lens with a bigger size is adopted. Therefore, the spot focused on PSD is strong enough and the PSD generates stable signals at low noise level. However, the mounting requirement limits the size of the lens. It is impossible to get a large lens in short focus without imaging distortion. The distance from the lens to the object is a major parameter affecting the light energy collected by the imaging lens. The smaller the distance, the more energy from the spot enters the imaging lens. In design, a diameter of 50mm plano-convex lens (focus 50mm) is utilized as the imaging lens. The distance from the lens to the pavement is set to 50mm (stand off distance). Therefore, the parameters in the formulas from Equation (3.1) through Equation (3.10) are $\alpha = 35°$, $L = 11$mm, $\alpha' = 40.038°$ and $L' = 91.034$mm respectively.

3.2 LASER BEAM

3.2.1 INTRODUCTION

Laser has had a tremendous impact on various fields in science and technology. It is now being widely used as a precise light source in medicine, communications, national defense, and measurement industries. Many types of lasers are commercially available with a large range of output wavelengths and power, such as HeNe, ruby, Nd-YAG, Nd-Glass, CO_2, dye, and the semiconductor diode.

Most laser systems are expensive and have complicated structures. The appearance of the laser diode can change this situation. Based on the features of the macro/micro measurement system, the low cost, small size, low power and simple-to-use semiconductor laser (laser diode) is adopted in the system.

3.2.2 FEATURES OF LASER

Lasers take many different forms and have many characteristics, such as wavelength, output power, duration of emission (pulsed or continuous), beam divergence, size and coherence.

Wavelength is a fundamental characteristic of the light. Each type of laser emits a characteristic wavelength. In the triangulation application, the visibility and detector-sensing range must be taken into account. A near infrared laser, with a wavelength of 780nm, is employed in the system. There are many reasons for choosing this laser. First of all, this characteristic wavelength is the closest to the sensitive peak of the PSD, which is 900nm. Secondly, the brightness of this infrared laser is not strong due to its characteristic wavelength near the scope of infrared band, which reduces the impairment to eyes. Thirdly, its visibility lets this semiconductor laser beam spot and the system is easy to be setup and aligned.

The output power is a major factor that affects the accuracy of the measurement system. In the triangulation method, the measurement is mainly implemented by the collection of reflected light intensity, which plays a critical role in the system. One of the system features that keep the received power constant is addressed. The function of this system is to solve the problem of uniform measurement on the surface with a different color and shape.

In the system, a continuous output laser is required. It is driven in the pulsed mode to meet the requirement of the special design of the measurement system.

3.2.3 LASER BEAM

The beam projected onto the surface must have a uniform intensity profile over the range of elevations to be measured. A single-mode laser beam and high-quality projection optics are required.

Like other laser diodes, it has the problem of divergence. A parallel beam is desired in the profiling measurement. To get an absolutely parallel beam, a complicated optical system needs to be built up. The shape of the laser source, the output power loss, the measurement accuracy and the simplicity should be considered with discernment.

Some trade-off should be reached. In our system design, a laser diode of 70mW, divergence of 0.49 and 5.6mm package (smaller light source) is chosen. It also has a good heat dissipation capability.
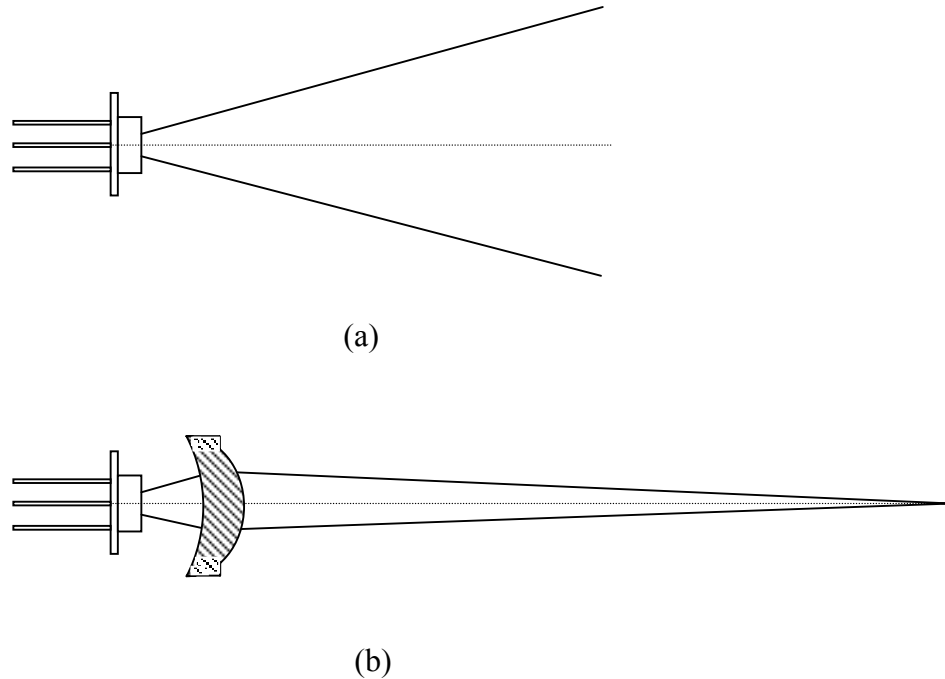

(a)

(b)

Figure 3.3 (a) Laser diode and beam divergence

(b) Beam collimation with an aspheric lens and focus

Figure 3.3 (a) illustrates the laser diode and the generation of the beam. The source of the laser diode is usually elliptical. A spherical lens cannot focus the divergent beam into an exact circular beam. Whereas, the aspherical lens can collimate the non-circular light source into an approximately circular beam if the light source is small and the focused distance is moderate. However, if a very high accuracy is required, an absolutely circular laser beam is definitely needed. A lens group should be combined to collimate the beam. For example, for a 250mW laser diode (9mm package), its source is a 2.0×0.3mm line shape, which needs an aspherical lens to focus the divergent lights into a line shape, and then another cylindrical lens is needed to focus the linear image into a circular spot (approximately). The level of complication of the lens grouping depends on the requirement of accuracy.

For this study, an aspherical lens is employed to generate the circular spot as shown in Figure 3.3 (b). Because the focus length is about 25cm and the measurement range is set to 20mm, an approximate circular beam can be obtained within that scope. The spot size is adjusted to about 0.4~0.7mm in diameter. It should be apparent that the diameter of the spot size should not be allowed to be arbitrarily too small. If the spot size is adjusted to a very small size, the surface texture will cause the detection system to be oversensitive to the micro texture. On the other hand, the larger spot size will not react to bigger particles due to blockage. However, if the spot size is too large, the fine texture will be ignored by the system. The surface range (position) with variable reflectivity within the laser spot size can result in intensity distributions (shift of the centroid). In this way, the finer displacement can be detected.

3.3 POSITION SENSING DETECTOR

Basically, there are two kinds of detectors suitable for high speed and high accuracy position-sensing detection: one is a couple charged device (CCD) and the other is a position sensitive detector (PSD).

3.3.1. CCD

CCD, used in triangulation measurement, can detect the peak value of the light quantity distribution of the beam spot focused on a CCD sensing array (linear) and then determine the precise target position.

CCD has its advantages and disadvantages. The advantages include the directly digitized output data, comparatively independent of light spot focus, and its easy process. The disadvantages include the low scanning rate and the limited resolution. For example, the linear scan CCD with the scanning rate 33MHz (256 pixels) has a reading rate of 128.9kHz. For the 33MHz scanning rate (512 pixels), its reading rate is 64.5kHz. For 40MHz (4096 pixels), its reading rate 9.76kHz. Only the 33MHz/256 pixels linear scan CCD meets our sampling rate requirement, i.e. 107kHz.

The CCD's pixel dimension is 14μm×14μm, which determines the smallest measurement resolution. It limits the extensibility of the measurement system. Furthermore, the total sensitive length of the 256-pixel line scan CCD is 256×14μm =

3.6mm, or a little bit longer, if considering the gaps between pixels. This sensitive length is another limitation on the measurement range.

3.3.2 PSD

The silicon opto-electronic sensor PSD can provide continuous position data of light spots traveling over their photosensitive surfaces. Compared to the discrete-element detectors, PSD has many advantages such as high position resolution (7μm), high-speed response time (0.7μs, i.e. 148kHz (5v) ~ 400kHz (15v)), and simultaneous measurements of position and intensity.

The PSD consists of monolithic, PIN (P, I and N layers) photodiodes with a uniform resistive surface. Figure 3.4 illustrates the principle of PSD.

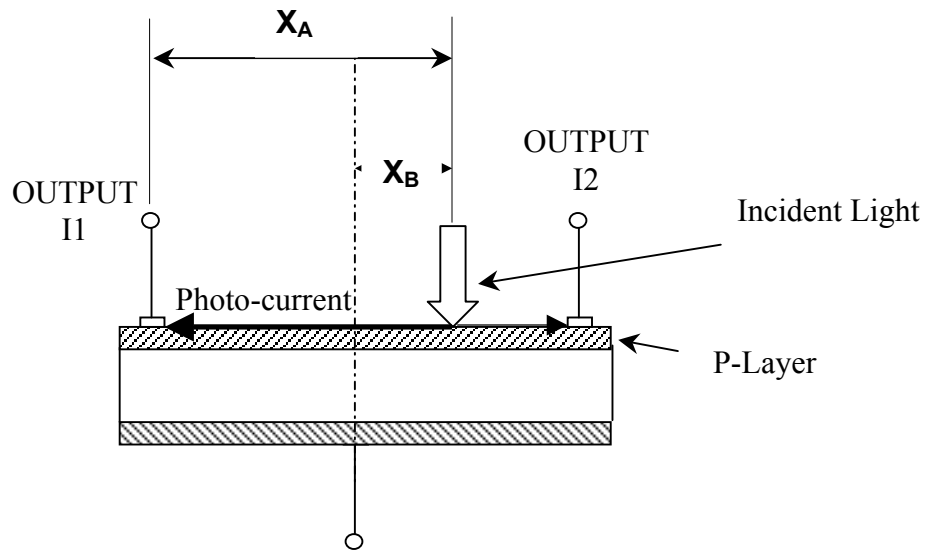Figure 3.4 PSD (position sensitive detector) principle diagram

When a light spot falls on the PSD, an electric charge proportional to the light energy is generated at the incident position. This electric charge is driven through the resistive P-layer and collected by the electrodes. Since the resistivity of the P-layer is uniform, the photocurrent collected by an electrode is inversely proportional to the

distance between the incident position and the electrode. It is possible to obtain the following formulas for the photo-currents *I1* and *I2* collected by the electrodes, where *L* and *I0* respectively stand for the electrode inter-distance and the total photo-current,

$$\frac{I_2 - I_1}{I_1 + I_2} = \frac{2x_A}{L} \tag{3.11}$$

or

$$x_A = \frac{L}{2} \times \frac{I_2 - I_1}{I_1 + I_2}. \tag{3.12}$$

From the difference or the ratio of *I1* and *I2,* the incident position of light can be found by the above formulas in respect to the energy of incident light [4]. The system circuit design is based on the above principle.

CHAPTER 4: MECHANICAL AND ELECTRICAL SYSTEM DESIGN AND SOFTWARE INTERFACE

4.1 LASER SCANNING SYSTEM DESIGN

In this device, a mechanical scanner controlled by a DC motor was designed. The nominal RPM number of the DC motor is 50, and the scanning speed for mechanical operation is around 2 Hz. The figure 4.1 is the mechanical scanner.

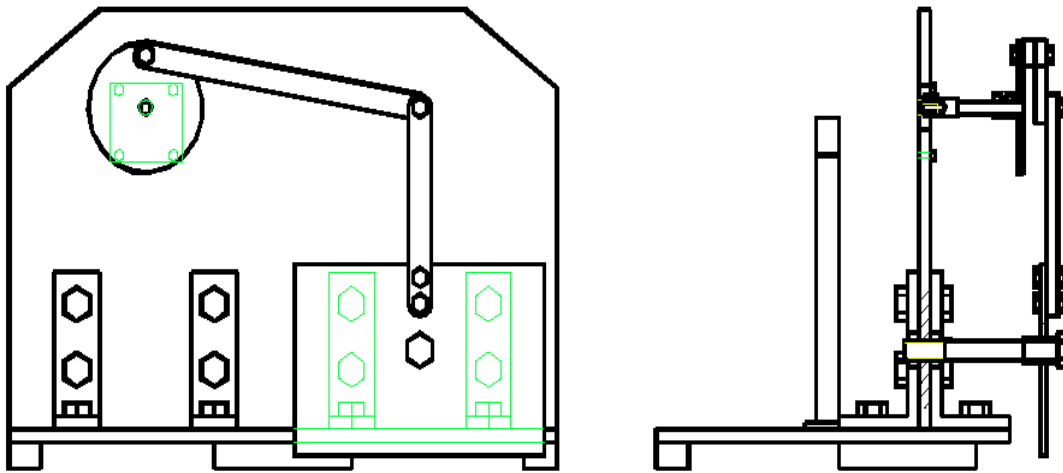Figure 4.1 Mechanical scanning systems

4.2 THE METHOD AND CORRESPONDING ALGORITHM TO DETERMINE THE MARKING THICKNESS

The design of the laser thickness-measuring device is intended to measure the thickness of the marking material. The average thickness of the marking material is defined as the average of the marking material and the base.

By using a mechanical scanning system and an angle encoder, a practical method was implemented to determine the thickness of the TPMM. The implementation is illustrated in Figure 4.2.
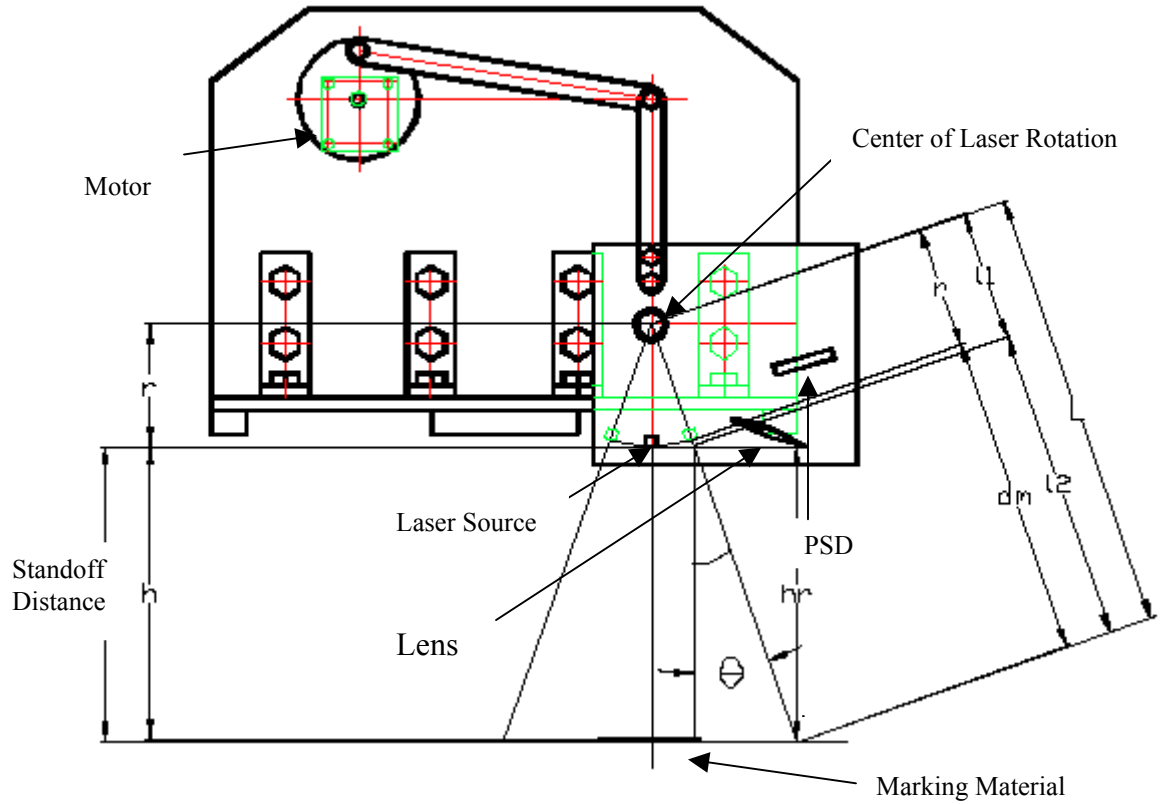
Figure 4.2. The mechanical scanning principle

In this method, the laser source is installed on a plate that rotates around a fixed center. When the motor starts to rotate at a 50-rpm speed, the laser beam can scan over the marking material at the speed of about 2 scans per second. The high-resolution encoder will measure the scan angle of the laser system. The corresponding algorithm is derived as the follows.

According to Figure 4.2, the following relationships can be established:

$$L = l_1 + l_2 = r + dm \tag{4.1}$$

$$l_1 = \frac{r}{\cos\theta} \tag{4.2}$$

Where r is the rotation radius of the laser source, dm is actually the measured linear distance between the laser source and the object, and θ is the rotation angle of the laser source. From Equations (4.1) and (4.2), l_2 can be expressed by Equation (4.3).

$$l_2 = (r + dm) - \frac{r}{\cos\theta} \qquad (4.3)$$

And from Figure 4.2, we can restore the relative height of the scanned position.

$$hr = l_2 \times \cos\theta = (r + dm) \times \cos\theta - r \qquad (4.4)$$

In this design, the rotation radius r is equal 3.57 inches, and the standoff distance is 12 inches.

By substituting the angle θ provided by the encoder into the above equations, we can process the data and restore the correct height of marking materials. The output signal of the data acquisition card is a voltage signal. The software uses the above equations to convert the voltage signal into height data, and then processes the height data. Finally the thickness information can be displayed on the computer screen. Figure 4.3 is the unprocessed voltage output from the data acquisition card. Figure 4.4 is the processed results that represent the thickness of marking materials. In Figure 4.3 and 4.4, X-axis is the counter number generated by the angle encoder that represents the scanning angle.
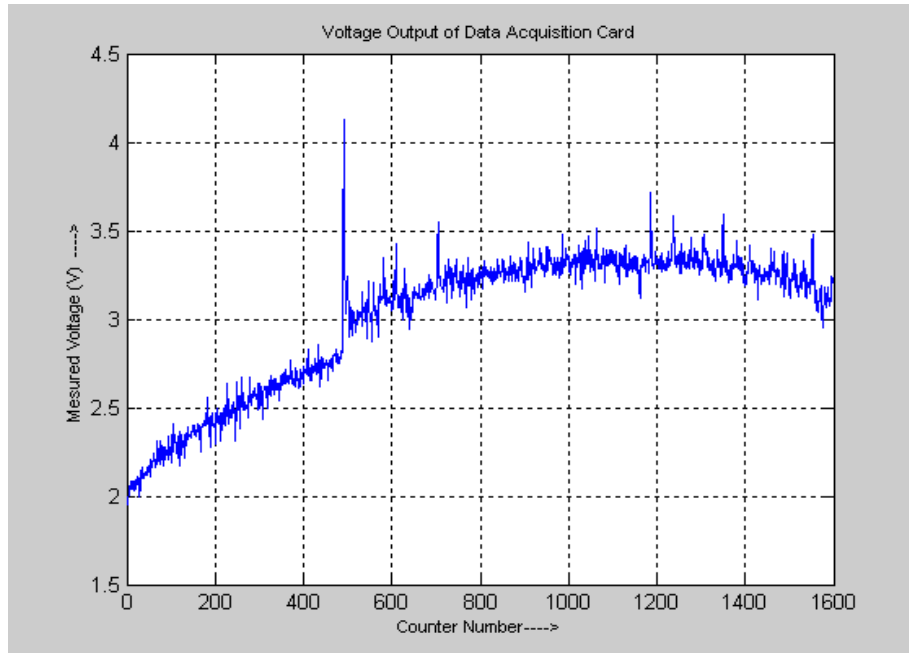
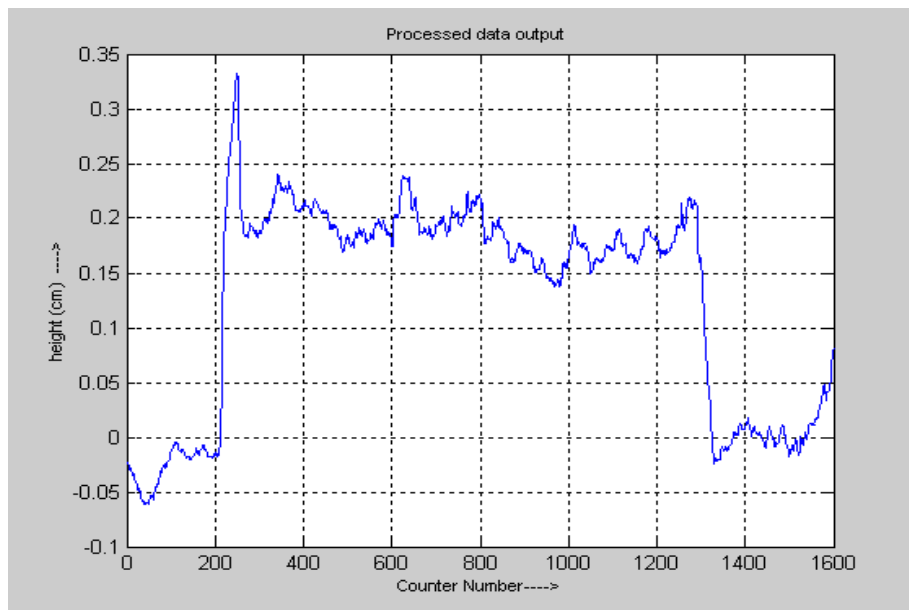Figure 4.3. The unprocessed voltage output from data acquisition card

Figure 4.4. The processed results that represent the thickness of marking materials

4.3. GPS SYSTEM

The GPS system provides position information where the measurement is conducted. Jupiter 11 is selected for the device, which is a twelve-channel GPS receiver module used for embedded applications. The following are the features of Jupiter 11:

- Twelve parallel channels for an "all-in-view" solution of the highest possible accuracy.

- 5.0 VDC or 3.3 VDC configurations.

- Options for fast acquisition or dead reckoning (use of aiding sensors).

- On-chip LNA supporting both active and passive antennas.

- Horizontal position accuracy of better than 2.8 meters SEP without differential aiding.

- Time accuracy of better than 100 ns to GPS or UTC time (user selectable).

- Optimized for the best possible acquisition and reacquisition in the harsh "urban canyon" environment.

- Proprietary algorithms maximizing tracking accuracy in high multipath environments.

- Low power consumption, 950 mW to 231 mW depending on configuration.

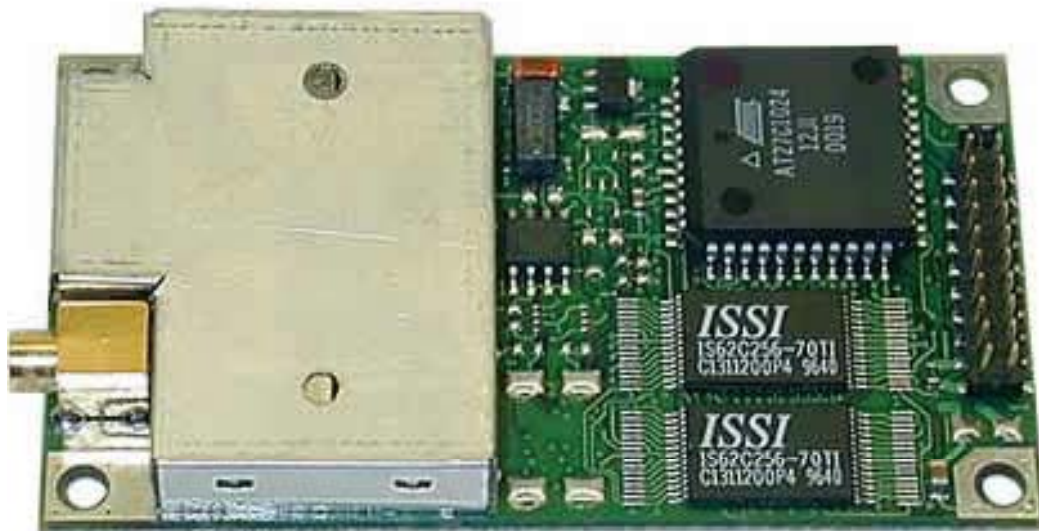- -40°C to +85°C thermal operating range.

Figure 4.5 Jupiter 11 GPS board

4.4 POWER SUPPLY

The power supply uses a 12V battery to provide voltages required by the devices to avoid AC input. Voltages from batteries are converted to required voltage by using a voltage regulator.

4.5 DATA ACQUISITION CARD

The Data Acquisition Card used in this project is National Instruments DAQCard-6062E. This high-performance interface card is connected to the PCMCIA (PC Card) slots of the laptop computer. The maximum sampling rate of this card is 500 ksps. The Data Acquisition Card has a resolution of 12-bit on all 16 single-ended analog inputs. In this design, 3 single-ended analog inputs are used for input signals.

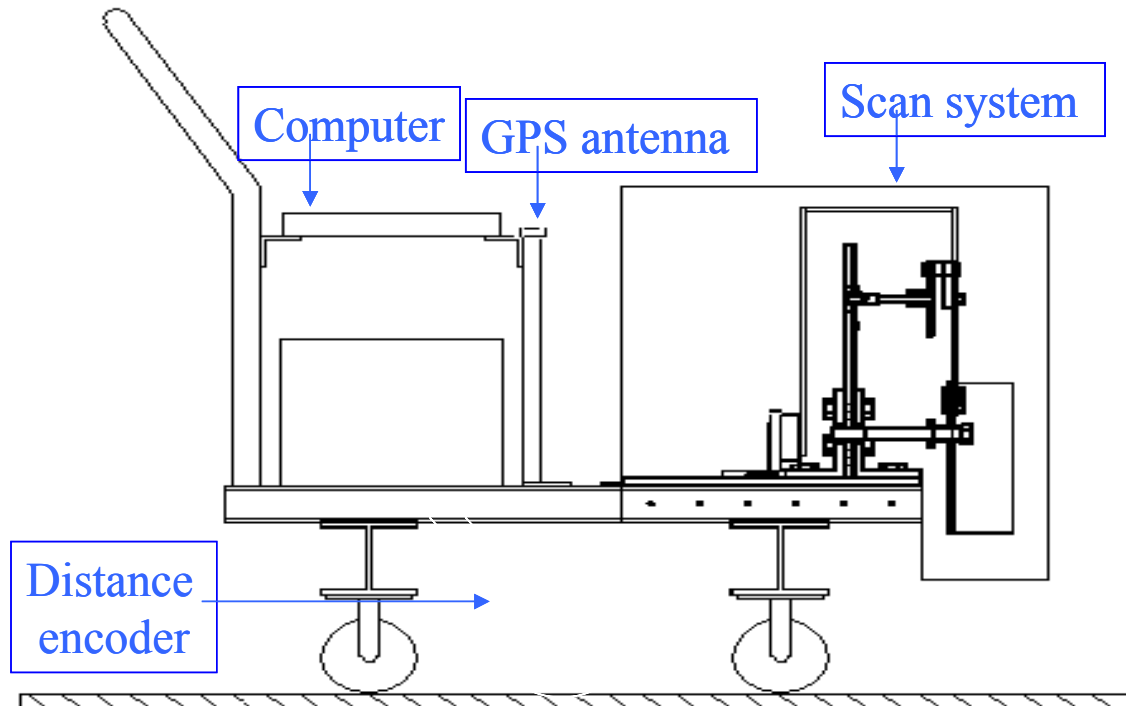The hardware configuration of the TPMM thickness device is shown in Figure 4.3.

Figure 4.6. The hardware structure of the TPMM thickness measurement device

4.6 SOFTWARE INTERFACE

The software package stores and processes the measured data. After the signal processing steps, the processed data, GPS position, and calculated average thickness can be displayed in real time. Figure 4.7 shows the software interface.

In the computer display, the GPS position of the starting point is recorded and displayed. Five traces of scanned results are displayed. Vertical axis is the distance from the laser source to the ground surface to be measured. On top of the display, the calculated average thickness of TPMM is displayed in centimeters. On the bottom of the display, the horizontal axis is the trace number measured.
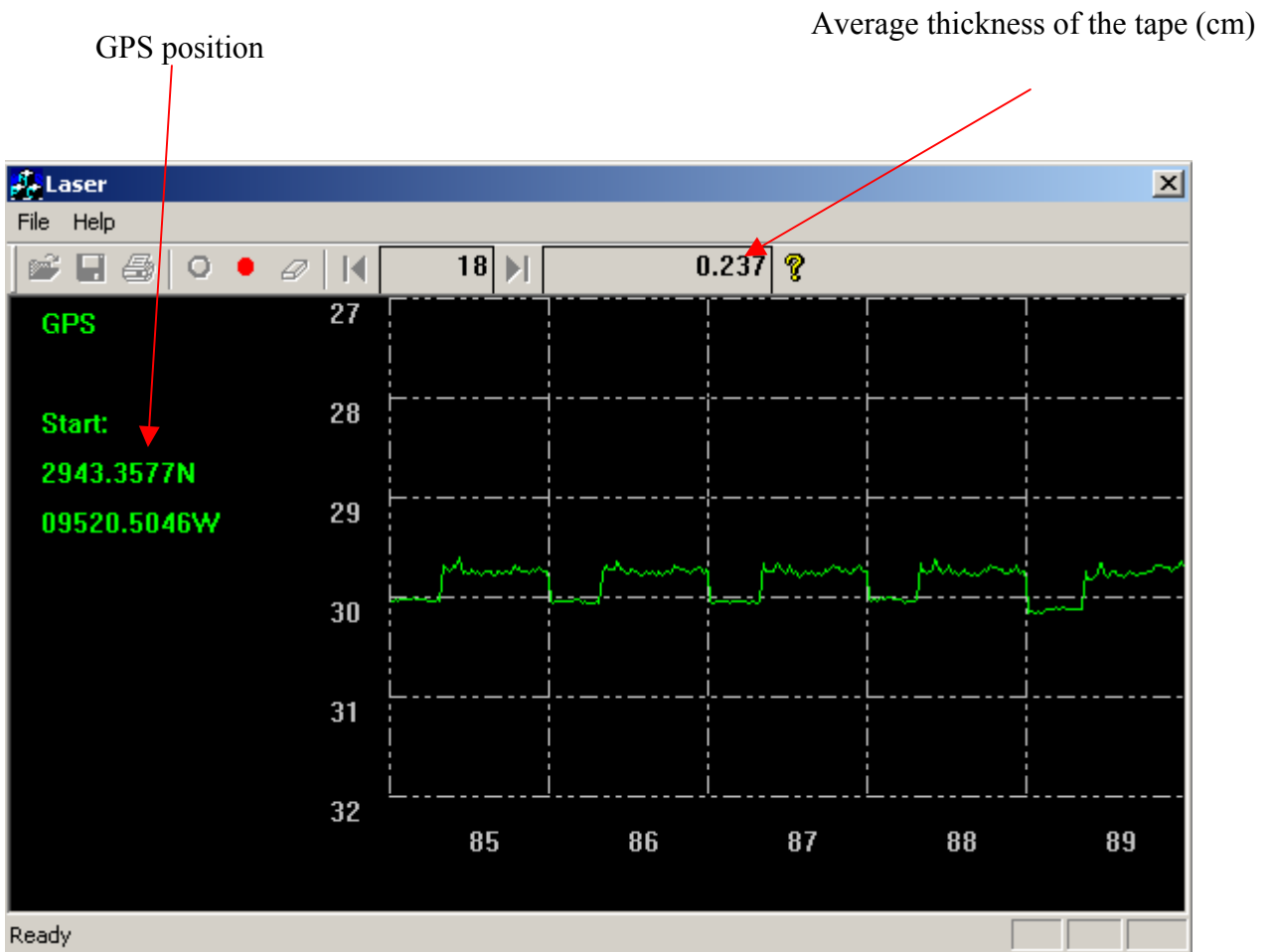

Figure 4.7 Software interface of the TPMM thickness device

CHAPTER 5: LAB AND FIELD TESTS

5.1 LAB TESTS

Various lab tests were done to verify the accuracy and robustness of this device. A calibration process was conducted using known object height. Due to the mechanical scanning, the measured signal is a curvature. The conversion process is described in a previous chapter. After data processing, the curvature is converted to the actual distance from the laser sensor to the surface of the TPMM. A typical measured trace is shown in Figure 5.1. Noises and spikes in Figure 5.1 are due to the sharp reflections from the surface of the glass beads on top of the TPMM.
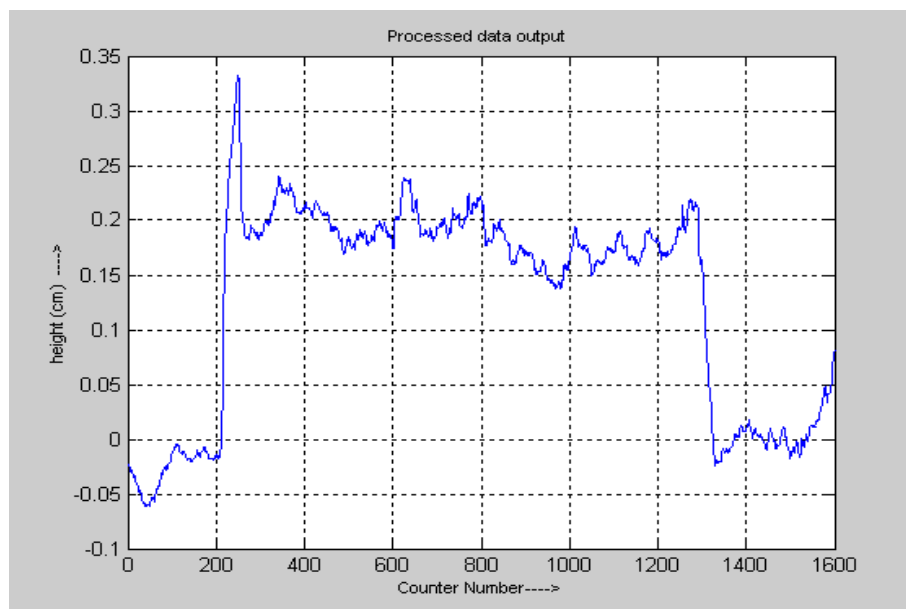
Figure 5.1 Measured TPMM thicknesses

Figure 5.2 shows the synchronization pulse collected from the laser system and used to indicate the location of the edge of the TPMM. For the case where the TPMM is placed on a flat surface, this signal is not very useful because it is very easy to find the location of the edge of the TPMM on the pavement by the laser device. However, on a rough surface, it is difficult to find the boundary point between the pavement and TPMM by the laser distance curve itself. To overcome this problem, the reflectivity signal available from the laser device is collected. This signal is sensitive to the reflectivity of

the target. Figure 5.2 shows the reflectivity signal measured on a TPMM over a rough surface. Figure 5.3 is the measured thickness data. Although the data shown in Figure 5.3 is very noisy due to the gravel, the edge of the tape can be easily detected using the reflectivity signal in Figure 5.2.
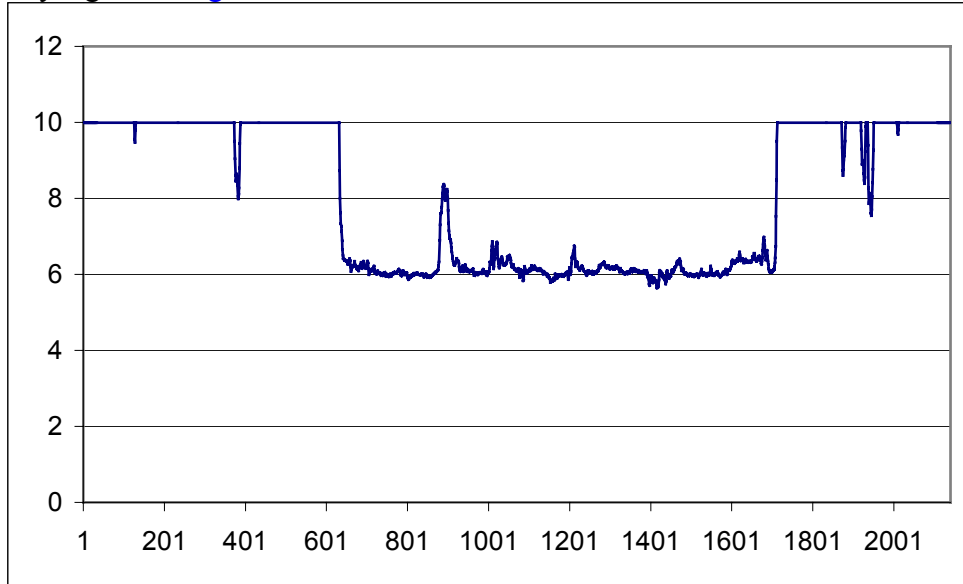
Figure 5.2 Reflectivity signal collected from the laser device. Horizontal axis is the trigger signal from angle encoder and vertical axis is the voltage.
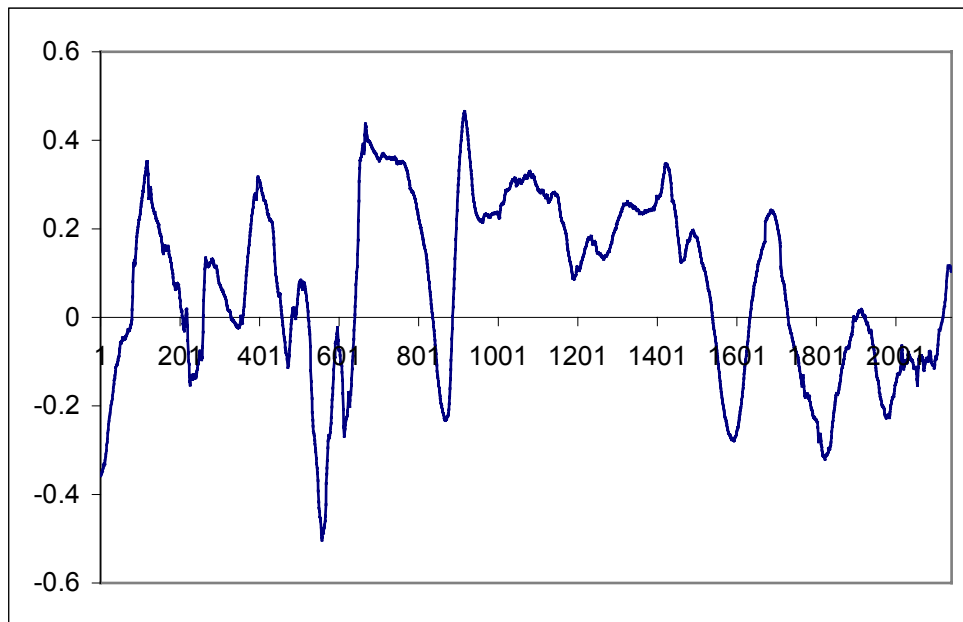
Figure 5.3 Measured TPMM thickness data over rough surface. Horizontal axis is the trigger signal from angle encoder and vertical axis is the voltage.

23

5.2 LAB SAMPLE PREPARATION

   Two types of lab samples were prepared. The first kind of sample was placed on a flat surface and the other was placed on gravel as shown in Figure 5.4. Colors of the sample were white and yellow both with 30% glass beads.

       (a)   (b)

Figure 5.4 (a) White sample on flat surface and (b) Yellow sample on gravel.

   During the lab tests it was found that the measurement of the TPMM thickness using the developed device is very accurate for a flat surface. Figure 5.5 shows the measurement of the TPMM over a flat surface.

Figure 5.5. Lab test over a flat pavement surface

However, measuring thickness of TPMM over gravel was difficult simply because the definition of "thickness" on a rough surface is hard. Due to the invasion of the melted TPMM when it was applied, some materials went into the porous area of the gravel reducing the effective thickness of the TPMM. Secondly, the measured laser data of TPMM over the gravel looks similar to those of the gravel without TPMM. Due to the random distribution of the gravel grains, the statistic average of the thickness of TPMM over gravel is defined as:

$$T_A = \frac{1}{N}\sum_{i=1}^{N}H_i - \frac{1}{M}\sum_{i=1}^{M}D_i \qquad (5.1)$$

Where T_A is the average thickness of the TPMM over gravel; N is the number of data points measured over TPMM in transverse direction; H_i is the ith distance data from laser device to TPMM surface; M is the number of data points measured over gravel surface next to the TPMM; Di is the ith distance data from laser device to gravel surface. Figure 5.6 (a) shows the picture of the TPMM over gravel. Figure 5.6 (b) shows the irregular shape of the TPMM peeled off the pavement after application.

(a)   (b)

Figure 5.6. (a) TPMM over rough pavement surface and (b) irregular thickness of TPMM

To verify the TPMM thickness measurement based on Equation (5.1), thickness measurement using the developed device is compared with data from a caliper as shown in Figure 5.6(b). Measured data using laser and caliper is listed in Table 5.1 and Table 5.2 respectively.

Table 5.1 Measured data by developed laser TPMM device (Unit: mil)

Groups / Times	1	2	3	4
1	66.46	60.22	97.78	52.70
2	76.74	69.11	53.05	82.18
3	69.2	106.0	61.57	69.15
4	71.28	69.82	45.16	83.10
5	76.79	57.41	95.28	56.95
6	77.08	82.30	69.63	77.53
7	89.29	72.40	90.48	110.0
8	67.36	82.31	68.80	10.5.0
9	92.49	106.0	77.49	47.94
10	81.28	115.0	75.39	85.01
Average	76.80	82.06	73.46	73.84

Table 5.2 Thickness measured by caliper (Unit: mil)

1	2	3	4	5	6	7	8	9	10	Average
74.8	76.8	78.7	64.96	68.89	78.74	76.8	72.83	66.93	80.71	74.02

Comparing the thickness data in Table 5.1 and Table 5.2, it is clearly seen that the average thickness of the TPMM measured by the laser TPMM device and caliper is very close.

5.3 FIELD TESTS

Organized by PD and PC, field tests were conducted in the Waco District on September 27, 2002. The purpose of the test is to test the accuracy of the developed TPMM thickness device over a rough pavement surface. In the test site, two different rough surfaces were found. The first kind is old asphalt pavement with smaller gravel as shown in Figure 5.7. The second is a newly laid asphalt pavement. In both cases, TPMM with the thickness of 100 mils before application was used. The TPMM is heated up using a heat gun during the application.

Figure 5.7. (a) Field-test in Waco District – TPMM over old asphalt pavement
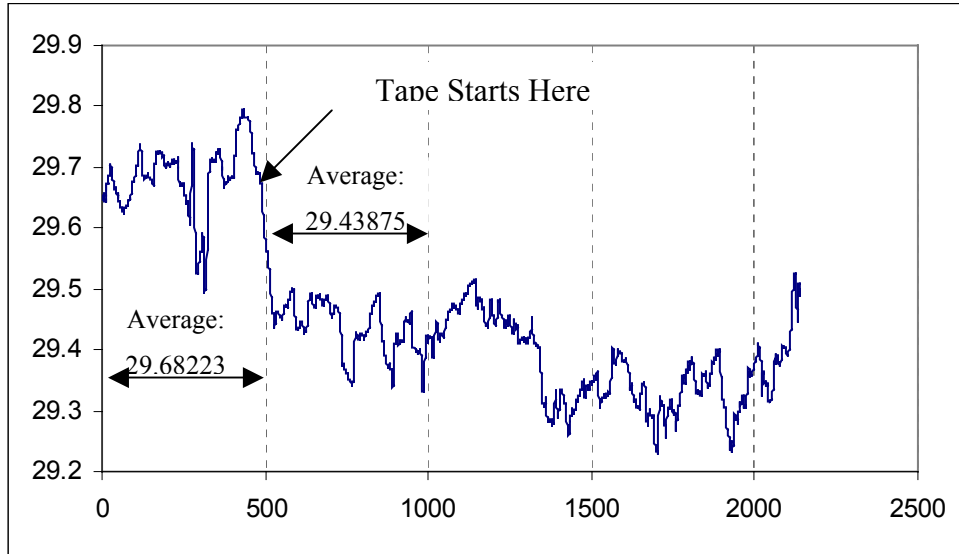
Figure 5.7 (b) Measured thickness profile of the TPMM over the old pavement in Waco

The horizontal axis is the number of samples in the transverse direction of the tape and the vertical axis is the distance in centimeters from the laser to the ground. In this figure, it is easy to tell the starting point of the tape material.

Using Equation (5.1), the average thickness of the TPMM is readily calculated to be 95.9 mils. Note that in this case, the computer can tell directly from the distance data where the TPMM and pavement edge is. However, in the new pavement shown in Figure 5.8 (a), the boundary is very difficult to find.

Figure 5.8 (a) Field test on new asphalt pavement

Figure 5.8 (b) TPMM on new pavement with rough surface in Waco District

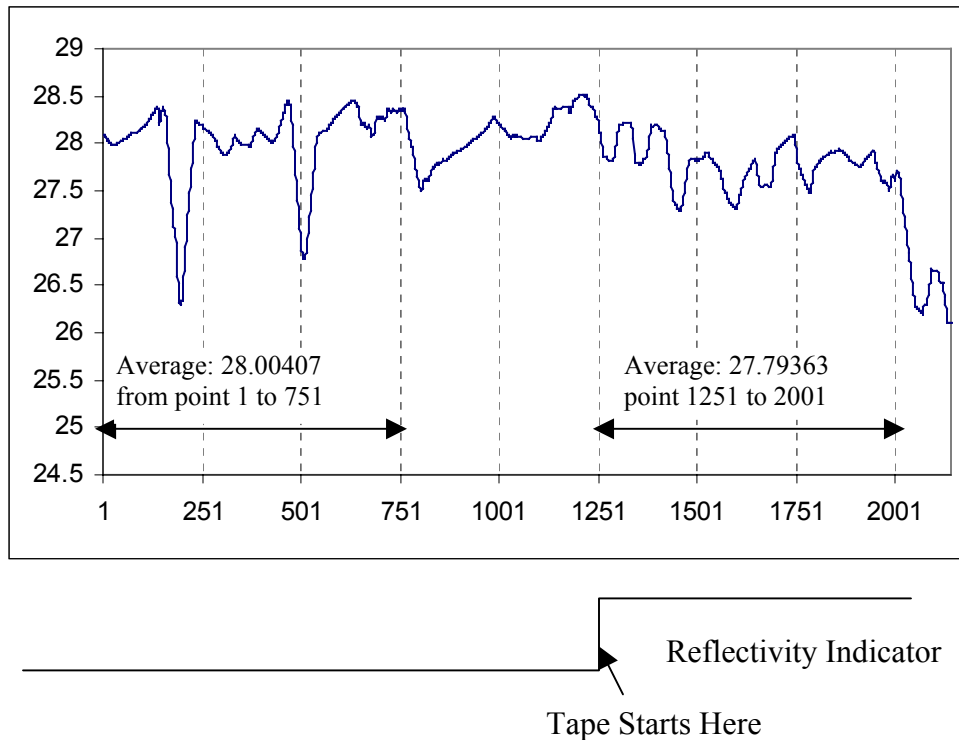Figure 5.8 (c) Relative gravel size used in Waco new pavement

Figure 5.8 (d) Measured thickness data using the laser TPMM thickness device

The horizontal axis is the number of samples in the transverse direction of the tape and the vertical axis is the distance in centimeters from the laser to the ground. In this figure, it is difficult to tell the starting point of the tape material without referencing to the reflectivity information shown at the bottom of the figure.

Using the reflectivity index, the computer program can easily find TPMM and pavement interface. By applying Equation (5.1), the TPMM thickness can be easily found to be 82.9 mils. Note that the thickness of TPMM over a rougher surface is thinner than that over a smoother surface. This result is expected because the high porosity of the rougher surface "eats" up some of the TPMM material.

CHAPTER 6: CONCLUSIONS AND RECOMMENDATIONS

6.1 CONCLUSIONS

In this project a laser thickness-measuring device for thermoplastic pavement marking material has been successfully developed. The developed hardware and software can measure TPMM thickness on concrete pavement and a rough pavement surface without contact. The prototype device was lab and field-tested. The test results show that the system can measure the thermoplastic thickness with satisfactory accuracy.

6.2 RECOMMENDATIONS

The researchers recommend the following:

1. The success of this project proves that non-contact TPMM measurement is feasible.

2. The product (thickness-measurement device) from this project has a high potential for   implementation.

3. To improve the implementation of this device some additional work must be done:

    a. Reduction in size of the pushcart.

    b. Redesign of the system for miniaturization.

    c. Replacement of the motor driven scanning with Galvanometer or acousto-optic deflection (AOD) scanning.

    d. Improvement of the thickness computation algorithm.

4. Initial results indicate a vehicle-mounted TPMM thickness measurement device can also be developed by building on the results from this project. An AOD device may be required and the computation algorithm will need to be modified to process the high volume of data. Use of a charged coupled device (CCD) camera with a scanning laser device may also be a potential method for TPMM thickness measurement.

REFERENCES

[1] Measuring and benefits, Selcom, Inc., No. 2, 1997.

[2] Bazin, G., Journal B, "A new laser range-finder based on FMCW-like method," IEEE Instrumentation and Measurement Technology Conference, June 4-6, 1996, pp. 90-93.

[3] Steel, W. H., "Interferometry," 2nd Ed., Cambridge University Press, New York, 1986.

[4] Dwulet, Robert J., "Laser triangulation expands measurement options," Design News, March 27, 1995, p. 114.

[5] Fair Lawn, "Laser sensor broadens sensing range," Design News, May 22, 1989, p. 42.

[6] Wiese, David R., "Laser triangulation sensors: a good choice for high speed inspection," I&CS, September, 1989, pp. 27-29.

[7] McCullough, Robert W. and Doyle, J. L., "Laser-optical triangulation systems provide new capabilities for remote inspection of interior surfaces," Materials Evaluation, December, 1995, pp. 1338-1345.

[8] Yakolev, V. V.,"High-precision laser range finders and laser systems for industrial use, Optical Engineering, August, 1994, Vol. 33, No. 8, pp. 2754-2758.

[9] Dalglish, R. L., McGarrity, C., and Restrepo, J., "Hardware architecture for real-time laser range sensing by triangulation," Rev. Scientific Instruments, Vol. 65, No. 2, February 1994, pp. 485-491.

[10] Opotcator Laser Sensor Manual, Selcom, Inc., 1996.

[11] Hamamatsu technical data about large-area PSD series, Hamamatsu Photonics K.K., 1993.

[12] Instruction Manual of Signal Processing Circuits for 1-dimensional PSD, Hamamatsu Photonics K.K.

[13] Tuerschmann, Mario, Mager, Peter P. and Endter, Rainer,"Improved accuracy in laser triangulation by variance-stabilizing transformations," Optical Engineering, July, 1992, Vol. 31, No. 7, pp. 1538-1545.

[14] Costa, Manuel F. M., "Surface inspection by an optical triangulation method," Optical Engineering, September, 1996, 39(9) pp. 2743-2747.

[15] Thomas,T. R., "Rough surfaces," Longman Group Limited, London and New York, 1982.

[16] Angelsky, Oleg V., "Interference measurement of rough surfaces," Simulation and Experiment in Laser Metrology, Akademie Verlag, Berlin, 1996, pp. 106-108.

[17] Beach, David, "Applications of lasers and laser system," PTR Prentice Hall, Englewood Cliffs, New Jersey, 1993.

[18] Hecht, Jeff, "Understanding lasers," IEEE Press, Understanding Science & Technology Series, New York, 1993.

[19] Palojarvi, Pasi, "Integrated time of flight laser radar," IEEE Instrumentation and Measurement Technology Conference, Brussels, Belgium, June 4-6, 1996.

[20] Domanski, Andrzelj W. and Wolinski, Tomasz R., "Surface roughness measurement with optical fibers," IEEE, 1992.

[21] Sayers, Michael W., "The Little Book of Profiling," University of Michigan, October, 1996.

[22] Mclean, J. and Foley, G., "Road surface characteristics and condition: effects on road users," ARRB Transport Research Ltd., Research Report No. 314.

[23] Luxon, James T. and Parker, David E., "Industrial lasers and their applications," Prentice-Hall, Inc., Englewood Cliffs, New Jersey, 1984.